J|A|C|S
ARTICLES
Published on Web 12/05/2006

Molecular Engineering of Organic Sensitizers for Solar Cell Applications

Sanghoon Kim,[†] Jae Kwan Lee,[†] Sang Ook Kang,[†] Jaejung Ko,*[,†] J.-H. Yum,[‡] Simona Fantacci,[§] Filippo De Angelis,[§] D. Di Censo,[‡] Md. K. Nazeeruddin,*[,‡] and Michael Grätzel*[,‡]

Contribution from the Department of Chemistry, Korea University, Jochiwon, Chungnam 339-700, Korea, Laboratory for Photonics and Interfaces, Station 6, Institute of Chemical Sciences and Engineering, School of Basic Sciences, Swiss Federal Institute of Technology, CH-1015 Lausanne, Switzerland, and Istituto CNR di Scienze e Tecnologie Molecolari (ISTM-CNR), c/o Dipartimento di Chimica, Università di Perugia, Via Elce di Sotto 8, I-06123 Perugia, Italy

Received September 3, 2006; E-mail: jko@korea.ac.kr; mdkhaja.nazeeruddin@epfl.ch; michael.graetzel@epfl.ch

Abstract: Novel organic sensitizers comprising donor, electron-conducting, and anchoring groups were engineered at molecular level and synthesized. The functionalized unsymmetrical organic sensitizers 3-{5-[*N*,*N*-bis(9,9-dimethylfluorene-2-yl)phenyl]-thiophene-2-yl}-2-cyano-acrylic acid (JK-1) and 3-{5′-[*N*,*N*-bis-(9,9-dimethylfluorene-2-yl)phenyl]-2,2′-bisthiophene-5-yl}-2-cyano-acrylic acid (JK-2), upon anchoring onto TiO_2 film, exhibit unprecedented incident photon to current conversion efficiency of 91%. The photovoltaic data using an electrolyte having composition of 0.6 M *M*-methyl-*N*-butyl imidiazolium iodide, 0.04 M iodine, 0.025 M LiI, 0.05 M guanidinium thiocyanate, and 0.28 M *tert*-butylpyridine in a 15/85 (v/v) mixture of valeronitrile and acetonitrile revealed a short circuit photocurrent density of 14.0 ± 0.2 mA/cm^2, an open circuit voltage of 753 ± 10 mV, and a fill factor of 0.76 ± 0.02, corresponding to an overall conversion efficiency of 8.01% under standard AM 1.5 sunlight. DFT/TDDFT calculations have been performed on the two organic sensitizers to gain insight into their structural, electronic, and optical properties. Our results show that the cyanoacrylic acid groups are essentially coplanar with respect to the thiophene units, reflecting the strong conjugation across the thiophene-cyanoacrylic groups. Molecular orbitals analysis confirmed the experimental assignment of redox potentials, while TDDFT calculations allowed assignment of the visible absorption bands.

Introduction

Dye-sensitized solar cells (DSCs) have attracted significant attention as low-cost alternatives to conventional solid-state photovoltaic devices.[1−12] These cells employ mostly ruthenium polypyridyl complexes as charge-transfer sensitizers, yielding over 11% solar-to-electric power conversion efficiencies in standard global air mass 1.5 sunlight.[13] To widen the choice for this critical component of the DSC, several groups have developed metal-free sensitizers and obtained efficiencies in the range of 5−8%.[14−18] There are several basic requirements guiding the molecular engineering of an efficient sensitizer. The excited-state redox potential should match the energy of the conduction band edge of the oxide. Light excitation should be associated with vectorial electron flow from the light-harvesting moiety of the dye toward the surface of the semiconductor surface providing for efficient electron transfer from the excited dye to the TiO_2 conduction band. Finally, a strong conjugation

[†] Korea University.
[‡] Swiss Federal Institute of Technology.
[§] ISTM-CNR Perugia.

(1) Special Issue: *Michael Graetzel Festschrift, A tribute for this 60th Birthday*: *Dye Sensitized Solar Cells*; Nazeeruddin, M. K., Ed.; Elsevier: Amsterdam, 2004; Vol. 248.
(2) Asbury, J. B.; Ellingson, R. J.; Gosh, H. N.; Ferrere, S.; Notzig, A. J.; Lian, T. *J. Phys. Chem. B* **1999**, *103*, 3110−3119.
(3) Park, N.-G.; Kang, M. G.; Kim, K. M.; Ryu, K. S.; Chang, S. H.; Kim, D.-K.; Van de Lagemaat, J.; Benkstein, K. D.; Frank, A. J. *Langmuir* **2004**, *20*, 4246−4253.
(4) Heimer, T. A.; Heilweil, E. J.; Bignozzi, C. A.; Meyer, G. J. *J. Phys. Chem. A* **2000**, *104*, 4256−4262.
(5) Lee, J.-J.; Coia, G. M.; Lewis, N. S. *J. Phys. Chem. B* **2004**, *108*, 5269−5281.
(6) Saito, Y.; Fukuri, N.; Senadeera, R.; Kitamura, T.; Wada, Y.; Yanagida, S. *Electrochem. Commun.* **2004**, *6*, 71−74.
(7) Kamat, P. V.; Haria, M.; Hotchandani, S. *J. Phys. Chem. B* **2004**, *108*, 5166−5170.
(8) Qiu, F. L.; Fisher, A. C.; Walker, A. B.; Petecr, L. M. *Electrochem. Commun*. **2003**, *5*, 711−716.
(9) Argazzi, R.; Larramona, G.; Contado, C.; Bignozzi, C. A. *J. Photochem. Photobiol., A* **2004**, *164*, 15−21.
(10) Bisquert, J.; Cahen, D.; Hodes, G.; Ruehle, S.; Zaban, A. *J. Phys. Chem. B* **2004**, *108*, 8106−8118.
(11) Figgemeier, E.; Hagfeldt, A. *Int. J. Photoenergy* **2004**, *6*, 127−140.
(12) Furube, A.; Katoh, R.; Yoshihara, T.; Hara, K.; Murata, S.; Arakawa, H.; Tachiya, M. *J. Phys. Chem. B* **2004**, *108*, 12588−12592.
(13) Nazeeruddin, M. K.; De Angelis, F.; Fantacci, S.; Selloni, A.; Viscardi, G.; Liska, P.; Ito, S.; Bessho, T.; Gra1tzel, M. *J. Am. Chem. Soc*. **2005**, *127*, 16835−16847.
(14) Hara, K.; Sato, T.; Katoh, R.; Furube, A.; Ohga, Y.; Shinpo, A.; Suga, S.; Sayama, K.; Sugihara, H.; Arakawa H. *J. Phys. Chem. B* **2003**, *107*, 597−606.
(15) Horiuchi, T.; Miura, H.; Sumioka, K.; Uchida, S. *J. Am. Chem. Soc*. **2004**, *126*, 12218−12219.
(16) Morandeira, A.; Boschloo, G.; Hagfeldt, A.; Hammarstrolm, L. *J. Phys. Chem. B* **2005**, *109*, 19403−19410.
(17) Ito, S.; Zakeeruddin, S. M.; Humphry-Baker, R.; Liska, P.; Charvet, R.; Comte, P.; Nazeeruddin, M. K.; Péchy, P.; Takata, M.; Miura, H.; Uchida, S.; Grätzel, M. *Adv. Mater*. **2006**, *18*, 1202−1205.
(18) Hagberg, D. P.; Edvinsson, T.; Marinado, T.; Boschloo, G.; Hagfeldt, A.; Sun, L. *Chem. Commun*. **2006**, 2245−2247.

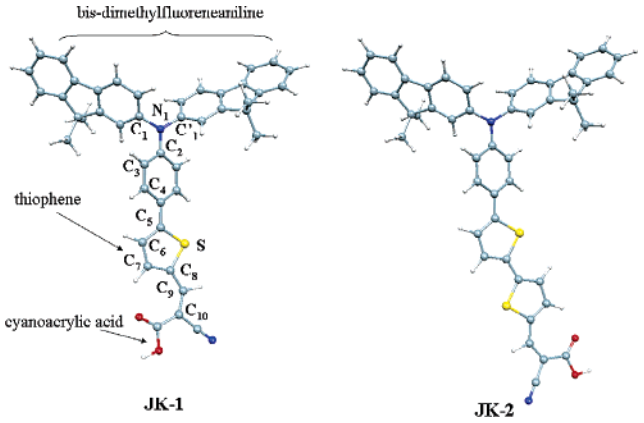

Figure 1. Optimized molecular structures of JK-1 and JK-2 by DFT calculations (see text for details). Atomic labels are also reported.

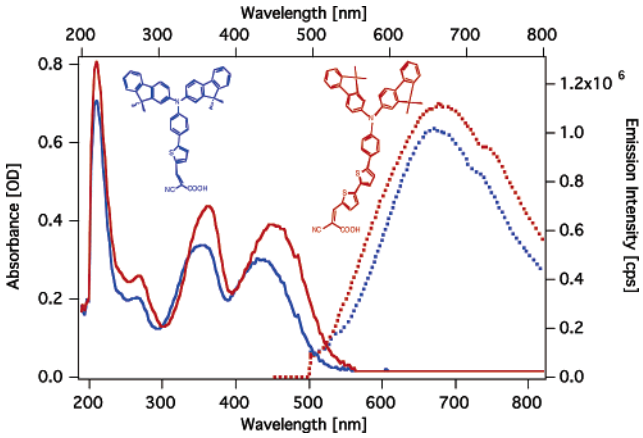

Figure 2. Absorption (solid lines) and emission (dashed lines) spectra of JK-1 (blue lines) and JK-2 (red lines) measured in EtOH solution. The emission spectra were obtained using the same solution by exciting at 450 nm at 298 K. The concentration for both solutions was 10^{-6} M. The insets show structures of JK1 (blue) and JK2 (red) sensitizers.

across the donor and anchoring groups and good electronic coupling between the lowest unoccupied orbital (LUMO) of the dye and the TiO_2 conduction band should exist, to ensure high electron-transfer rates.

A major factor for the low conversion efficiency of many organic dyes in the DSC is the formation of dye aggregates on the semiconductor surface. Such an aggregation phenomenon would affect the light absorption by filtering effect.[19] Therefore, for obtaining optimal performance, aggregation of organic dyes needs to be avoided through appropriate structural modification.[20] Another important issue for organic dyes is their stability, which is generally lower than that of metal complexes, likely bleeding channels being the formation of excited triplet states and unstable radicals.[21]

To incorporate these required properties, we have designed and synthesized the novel unsymmetrical organic sensitizers JK-1 and JK-2 (see Figure 1) that consist of the bis-dimethylfluoreneaniline moiety acting as electron donor and cyanoacrylic acid moiety acting as acceptor, the two functions being connected by conducting thiophene units. The tailored dimethylfluoreneaniline moieties in the JK-1 and JK-2 sensitizers ensure greater resistance to degradation when exposed to light and high temperatures as compared to simple arylamines. Also, the nonplanar structure of dimethylfluoreneaniline suppresses aggregation, disfavoring molecular stacking. Finally, the bridging thiophene units are used to provide conjugation between the donor and the anchoring groups as well as to increase the molar extinction coefficient of the dye.[22] Herein, we report on the synthesis, characterization, and photovoltaic properties of the two sensitizers JK-1 and JK-2. Moreover, we perform DFT/TDDFT calculations to provide a detailed characterization of the structural, electronic and optical properties of the two sensitizers.

Results and Discussion

The functionalized unsymmetrical sensitizers 3-{5-[*N*,*N*-bis(9,9-dimethylfluorene-2-yl)phenyl]-thiophene-2-yl}-2-cyanoacrylic acid (JK-1) and 3-{5′-[*N*,*N*-bis(9,9-dimethylfluorene-2-yl)phenyl]-2,2′-bisthiophene-5-yl}-2-cyano-acrylic acid (JK-2) were conveniently synthesized by reacting the 5-[*N*,*N*-bis(9,9-dimethylfluorene-2-yl)phenyl]-thiophene-2-carbaldehyde and 3-{5′-[*N*,*N*-bis(9,9-dimethylfluorene-2-yl)phenyl]-2,2′-bisthiophene-5-yl}-5-carbaldehyde with cyanoacetic acid in acetonitrile in the presence of piperidine, respectively (see synthetic section for details).

Figure 2 shows the UV/vis spectra of the JK-1 and JK-2 sensitizers measured in ethanol solution. The absorption spectrum of JK-1 displays two visible bands at 354 nm ($\epsilon = 34\,000$ $dm^3\ mol^{-1}\ cm^{-1}$) and 436 nm ($\epsilon = 30\,000$ $dm^3\ mol^{-1}\ cm^{-1}$), which are due to the $\pi-\pi^*$ transitions of the conjugated molecule; see TDDFT calculations below. Under similar conditions, the JK-2 sensitizer that contains two thiophene units exhibits absorption bands at 364 nm ($\epsilon = 44\,000$ $dm^3\ mol^{-1}\ cm^{-1}$) and at 452 nm ($\epsilon = 39\,000$ $dm^3\ mol^{-1}\ cm^{-1}$) that are red-shifted as compared to the JK-1 sensitizer. Both compounds show a strong band in the UV region at 210 nm ($\epsilon \approx 80\,000$ $dm^3\ mol^{-1}\ cm^{-1}$). The absorption spectra of JK-1 and JK-2 adsorbed onto 2 μm thick TiO_2 electrodes are similar to those of the corresponding solution spectra but exhibit a small red-shift due to the interaction of the anchoring groups with the surface titanium ions. When the JK-1 and JK-2 sensitizers are excited within their $\pi-\pi^*$ within bands in an air-equilibrated solution at 298 K, they exhibit strong luminescence maxima at ~657 and 670 nm, respectively.

Electrochemical properties of the JK-1 and JK-2 sensitizers were scrutinized by cyclic voltammetry in propylene carbonate solvent containing 0.1 M tetrabutylammonium tetrafluoroborate. TiO_2 films stained with sensitizer were used as working electrodes. The JK-1 dye adsorbed on TiO_2 films shows a reversible couple at 1.16 V vs NHE with a separation of 0.15 V between anodic and cathodic peak, which is due to the oxidation of 3-{5-[*N*,*N*-bis(9,9-dimethylfluorene-2-yl)phenyl] group (Figure 3). Under similar conditions, the JK-2 dye shows two redox processes located at 1.04 and 1.47 V vs NHE, respectively. Analysis of the first reversible process in both dyes shows the oxidation potentials are very close, due to the similar donor groups. The second redox process in JK-2 is likely due to the oxidation of dithiophene unit, which is absent in JK-1 within the measured electrochemical window.

(19) Liu, D.; Fessenden, R. W.; Hug, G. L.; Kamat, P. V. *J. Phys. Chem. B* **1997**, *101*, 2583−2590.
(20) Burfeindt, B.; Hannappel, T.; Storck, W.; Willig, F. *J. Phys. Chem.* **1996**, *100*, 16463−16465.
(21) Sayama, K.; Tsukagoshi, S.; Hara, K.; Ohga, Y.; Shinpou, A.; Abe, Y.; Suga, S.; Arakawa, H. *J. Phys. Chem. B* **2002**, *106*, 1363−1371.
(22) Hara, K.; Kurashige, M.; Dan-oh, Y.; Kasada, C.; Shinpo, A.; Suga, S.; Sayama, K.; Arakawa, H. *New J. Chem.* **2003**, *27*, 783−785.

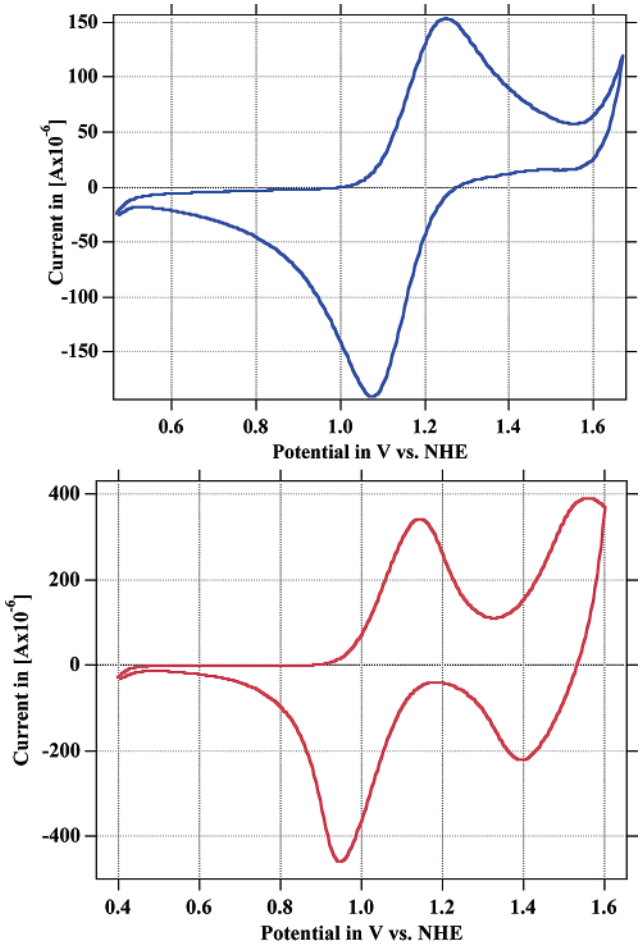

Figure 3. Cyclic voltammetry of JK-1 (top panel) and JK-2 sensitizers (bottom panel) attached to a nanocrystalline TiO_2 film deposited on conducting FTO glass (electrode size 0.28 cm^2, film thickness 2.5 μm, particle size 20 nm). The film was sintered at 450 °C for 20 min. After 10 min of cooling, it was immersed in the dye solution overnight. The sensitized electrodes were washed with pure acetonitrile and measured under inert atmosphere in a glove box with a scan rate of 100 mV s^{-1}.

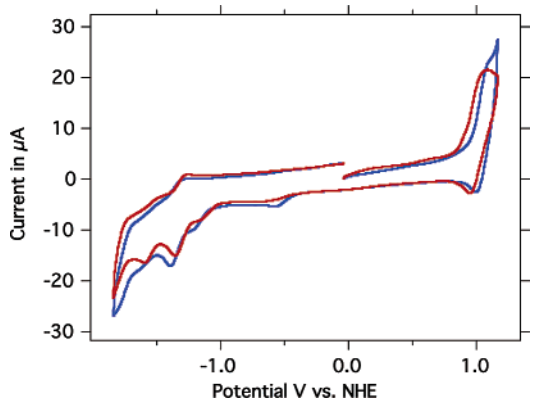

Figure 4. Cyclic voltammogram of the JK-1 (blue line) and JK-2 (red line) measured in a DMF solution containing 0.1 M TBA(PF_6) using a glassy carbon as a working and a Pt counter electrode with a scan rate of 100 mV s^{-1}.

Figure 4 shows the cyclic voltammogram of JK-1 and JK-2 obtained in DMF solution using 0.1 M tetrabutylammonium hexafluorophosphate tetrabutyl as a supporting electrolyte and a glassy carbon working electrode. Both dyes exhibited a quasi-reversible wave at 1.06 and 1.01 V vs NHE, which are assigned again to the oxidation of the 3-{5-[*N*,*N*-bis(9,9-dimethylfluorene-2-yl)phenyl]. When scanning toward negative potentials, the two sensitizers showed quasi-reversible wave at $E_{1/2} = -1.34$ and -1.30 V, respectively (see Figure 4). The positive shift of the first reduction potential in JK-2 as compared to that of JK-1 is due to extension of the π-conjugation, in keeping with the theoretical analysis presented below.

To gain insight into the geometrical, electronic, and optical properties of the JK-1 and JK-2 dyes, we performed DFT calculations on the two organic sensitizers and time-dependent DFT (TDDFT) calculations of the excited states for JK-1, using the Gaussian 03 program package.[25] In particular, we used the B3LYP exchange-correlation functional[26] and a 6-31g* basis set;[27] solvation effects were included by means of the polarizable continuum model.[28] We optimized the molecular structure of JK-1 and JK-2 in the gas phase without any symmetry constraints, obtaining the geometries shown in Figure 1. It is worth noting that for both the JK-1 and the JK-2 optimized structures we calculate the two dimethyl-fluorene ligands bound to the aniline N_1, to arrange in an out-of-plane fashion (see Figure 1) to minimize the steric hindrance, as reflected by the calculated value of the $-C_1(C'_1)-N_1-C_2-C_3$ dihedral angles of 31.6−31.4° and 34.1−33.7°, for JK-1 and JK-2, respectively. The angle formed between the aniline and the thiophene planes is computed to be 20.5° and 22.7° in JK-1 and JK-2 complexes, respectively, while the cyanoacrylic acid group was found to be essentially coplanar with respect to the thiophene unit, reflecting the strong conjugation across the thiophene-cyanoacrylate groups. We also notice that in the JK-2 case the two thiophene units are essentially coplanar, both considering a cisoid and transoid arrangement of the two ligands, the latter being favored by only 0.7 kcal/mol.

We then analyzed the electronic structure of both organic sensitizers in vacuo and in ethanol solution, which is the solvent used to record the experimental spectra. A schematic representation of the molecular orbital energies is reported in Figure 5, while in Figure 6 we report the isodensity plots of the frontier molecular orbitals of JK-1. The highest occupied molecular orbital (HOMO) of the two sensitizers, both in vacuo and in solution, is delocalized over the bis-dimethyl-fluoreneaniline ligand, with maximum components arising from the nitrogen lone-pair and the π framework of the surrounding ligands; the HOMO-1 is, on the other hand, a π-bonding orbital delocalized over the entire molecule, with maximum components on the thiophene and cyanoacrylic moieties; see Figure 6. The lowest unoccupied molecular orbital (LUMO) is for both sensitizers a π^* orbital delocalized across the thiophene and cyanoacrylic groups, with sizable components from the cyano- and carboxylic moieties; the LUMO+1 is a π^* orbital of the two dimethyl-fluorene ligands; see Figure 6.

Inspection of the frontier orbitals of JK-1 and JK-2 reveals that the HOMO and LUMO of both species are essentially

(23) Nazeeruddin, M. K.; Pećhy, P.; Renouard, T.; Zakeeruddin, S. M.; Humphry-Baker, R.; Comte, P.; Liska, P.; Le, C.; Costa, E.; Shklover, V.; Spiccia, L.; Deacon, G. B.; Bignozzi, C. A.; Grätzel, M. *J. Am. Chem. Soc.* **2001**, *123*, 1613−1624.
(24) Wang, P.; Zakeeruddin, S. M.; Comte, P.; Charvet, R.; Humphry-Baker, R.; Grätzel, M. *J. Phys. Chem. B* **2003**, *107*, 14336−14341.
(25) Frisch, M. J.; et al. *Gaussian 03*, revision B.05; Gaussian, Inc.: Wallingford, CT, 2004.
(26) Becke, A. D. *J. Chem. Phys.* **1993**, *98*, 5648−5652.
(27) Ditchfield, R.; Herhe, W. J.; Pople, J. A. *J. Chem. Phys.* **1971**, *54*, 724.
(28) (a) Barone, V.; Cossi, M. *J. Phys Chem. A* **1998**, *102*, 1995−2001. (b) Cossi, M.; Rega, N.; Scalmani, G.; Barone, V. *J. Comput. Chem.* **2003**, *24*, 669−681.

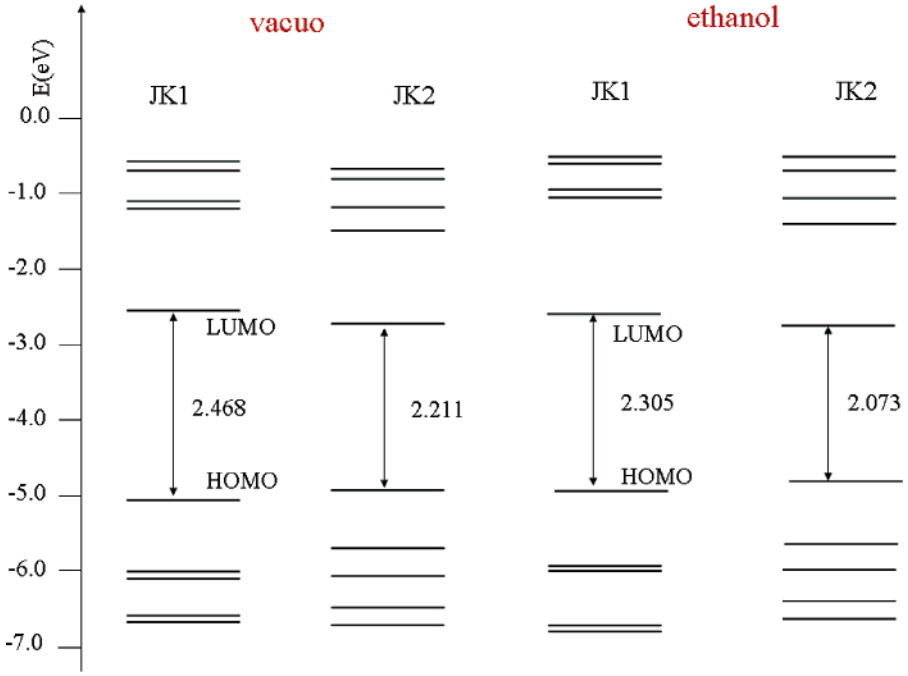

Figure 5. Schematic representation of the frontier molecular orbitals of JK-1 and JK-2 in vacuo and in ethanol.

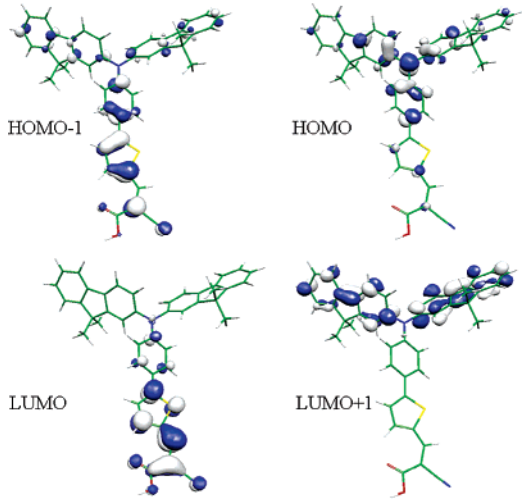

Figure 6. Isodensity surface plots of the HOMO−1, HOMO, LUMO, and LUMO+1 of JK-1. Similar orbitals are calculated for JK-2.

isolated orbitals in energy, with the HOMO−1 and LUMO+1 lying ca. 1 eV below and above the HOMO and LUMO, respectively. It is interesting to notice that the HOMO and LUMO of JK-2 are destabilized and stabilized by 0.10 and 0.16 eV, respectively, as compared to the corresponding JK-1 orbitals. As a result, the JK-2 HOMO−LUMO gap reduces to 2.21 eV, as compared to 2.47 eV calculated for JK-1, with the sizable LUMO stabilization being due to the increased conjugation along the ligand due to the presence of a second thiophene unit. Inclusion of solvation effects does not lead to a qualitative change in the electronic structure picture discussed above, even though smaller HOMO−LUMO gaps are calculated as compared to the gas phase, mainly because of the HOMO destabilization taking place in solution; see Figure 5.

It is worth comparing our calculated electronic structure to the available electrochemical and spectroscopic data obtained in the context of the present investigation. We notice that the trend of calculated HOMO−LUMO gaps nicely compares with the spectroscopic data, showing a red-shift of the absorption maximum in going from JK-1 to JK-2. Also, the electrochemical oxidation and reduction potential data are consistent with the trends in the calculated HOMOs and LUMOs energies for the two dyes, showing an increase (decrease) of the HOMO (LUMO) energies in going from JK-1 to JK-2, which nicely correlates with the small negative (positive) shifts measured for the oxidation (reduction) processes.

Table 1. Calculated TDDFT Excitation Energies (eV, nm), Oscillator Strengths (*f*), Composition in Terms of Molecular Orbital Contributions, and Character, As Compared to Experimental Absorption Band Maxima[a]

n	*E* (eV, nm)	*f*	composition	character	exp.
1	2.23 (555)	0.71	89% HOMO → LUMO	CT	2.84 (436)
2	3.20 (387)	0.79	74% HOMO−1 → LUMO	$\pi-\pi^*$ (1)	3.50 (354)
4	3.37 (368)	0.61	88% HOMO → LUMO+1	$\pi-\pi^*$ (2)	

[a] *n* is the ordering number of the calculated excited state.

To gain insight into the excited states giving rise to the intense absorption bands exhibited by the two sensitizers, we performed TDDFT excited states calculations at the B3LYP/6-31G* level. Given the negligible effect of solvation on the electronic structure, TDDFT calculations were performed in vacuo and were limited to JK-1. In the TDDFT calculations, the lowest 10 singlet−singlet excitations were calculated, up to an energy of ca. 4 eV (310 nm). Within the considered energy range, we calculate three transitions of sizable intensity ($f > 0.1$), whose energies, oscillator strengths, and composition in terms of molecular orbital contributions[29] are reported in Table 1.

The lowest transition is calculated at 2.23 eV and corresponds to a charge-transfer (CT) excitation from the bis-dimethylfluoreneaniline-based HOMO to the LUMO, localized on the thiophene-cyanoacrylate moieties. As compared to the experimental absorption maximum, found at 2.84 eV, the calculated transition is considerably red-shifted. This is related to the extended charge-transfer character of this transition, which is

not properly captured by TDDFT calculations employing current exchange-correlation functionals.[30] The band experimentally found at 3.50 eV (354 nm) appears to be composed by two almost overlapping $\pi-\pi^*$ transitions of different character, calculated at 3.20 and 3.37 eV, (1) and (2) in Table 2, respectively. The transition calculated at 3.20 eV is a $\pi-\pi^*$ excitation from the HOMO−1 to the LUMO, therefore taking place within the thiophene-cyanoacrylate moiety. The slightly less intense transition calculated at 3.37 eV is, on the other hand, a $\pi-\pi^*$ excitation from the HOMO to the LUMO+1, corresponding therefore to excitation within the bis-dimethylfluoreneaniline moiety. The better agreement between the calculated and experimental absorption energies of the $\pi-\pi^*$ features as compared to the CT excitation is related to the localized character of the $\pi-\pi^*$ excitations, which involve substantially overlapping orbitals.

The excited-state oxidation potential of the sensitizer plays an important role in the electron injection process. Neglecting any entropy change during light absorption, the value can be derived from the ground-state oxidation couple and the zero−zero excitation energy $E^{(0-0)}$ according to eq 1.

$$E(S^+/S^*) = E(S^+/S) - E^{(0-0)} \quad (1)$$

From the emission spectra, $E^{(0-0)}$ energies of 2.43 and 2.37 eV were extracted for JK-1 for JK-2, respectively. The excited-state oxidation potentials of the two sensitizers JK-1 and JK-2 are −1.27 and −1.36 V vs NHE, respectively, which are notably more negative than the equivalent potential for N719 dye (−0.98 V vs NHE) and the TiO_2 conduction band.[14] Therefore, this type of sensitizer could become very attractive, particularly for semiconductor materials having Fermi levels more negative than TiO_2, where an increased gap between the conduction band and the redox couple will result in a higher open-circuit potential enhancing the cell efficiency considerably. On the other hand, the oxidation potentials of the two sensitizers are more positive than the I^-/I_3^- redox couple (∼0.4 V vs NHE), ensuring that there is enough driving force for the dye regeneration reaction to compete efficiently with recapture of the injected electrons by the dye cation radical.

Both sensitizers have been used to manufacture solar cell devices to explore current−voltage characteristics using 10 + 4 μm TiO_2 transparent layers. The screen-printed double layer films, consisting of a 10 μm transparent layer and a 4 μm scattering layer, were prepared and treated with 40 mM titanium tetrachloride solution using a previously reported procedure.[13,23] The TiO_2 electrodes were immersed into the JK-1 and JK-2 solutions (0.5 mM in a mixture of acetonitrile and *tert*-butyl alcohol (volume ratio: 1:1) containing 1 mM 3a,7a-dihydroxy-5b-cholic acid (Cheno)) and kept at room temperature for 4 h.

(29) Characterization of the nature of the TDDFT transitions in terms of single orbital excitations is usually possible, provided one has access to the eigenvectors. The latter are made up of two component vectors, *X* and *Y*, related to single-particle excitations and de-excitations, respectively. In G03, however, the program only provides the (dominant) components of the sum vector $X + Y$, and it is thus impossible in principle to separate the interfering excitation and de-excitation components. To the extent, however, that we may reasonably assume that the de-excitation vector *Y* is small as compared to *X* (it would exactly be zero in the Tamm−Dancoff or single excitation CI approximation), we may take the square of the $X + Y$ vector components as a qualitative measure of the weight pertaining to the corresponding single excitations.

(30) (a) Dreuw, A.; Head-Gordon, M. *J. Am. Chem. Soc.* **2004**, *126*, 4007. (b) Tozer, D. J.; Amos, R. D.; Handy, N. C.; Roos, B. O.; Serrano-Andres, L. *Mol. Phys.* **1999**, *97*, 859.

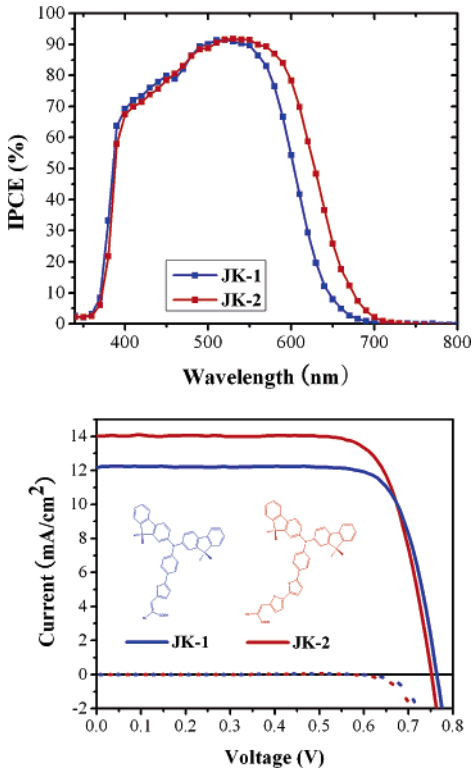

Figure 7. IPCE (top) and current−voltage characteristics (bottom) obtained with a nanocrystalline TiO_2 film supported on FTO conducting glass and derivatized with monolayer of JK-1 (blue line) and JK-2 (red line). A sandwich-type cell configuration was used to measure this spectrum. The redox electrolyte was comprised of 0.6 M *M*-methyl-*N*-butyl imidiazolium iodide, 0.04 M iodine, 0.025 M LiI, 0.05 M guanidinium thiocyanate, and 0.28 M *tert*-butylpyridine in a 15/85 (v/v) mixture of valeronitrile and acetonitrile.

The stained TiO_2 electrode and Pt-counter electrode were assembled into a sealed sandwich-type cell by heating with a hot-melt ionomer film (Surlyn 1702, 25 μm thickness, Du-Pont) as a spacer between the electrodes.[13]

Figure 7 shows the incident monochromatic photon-to-current conversion efficiency (IPCE) obtained with a sandwich cell using 0.6 M *M*-methyl-*N*-butyl imidiazolium iodide, 0.04 M iodine, 0.025 M LiI, 0.05 M guanidinium thiocyanate, and 0.28 M *tert*-butylpyridine in a 15/85 (v/v) mixture of valeronitrile and acetonitrile as redox electrolyte. The IPCE data of both JK-1 and JK-2 sensitizers plotted as a function of excitation wavelength exhibit a strikingly high plateau at 91%. The JK-2 sensitizer IPCE spectrum is red-shifted by about 30 nm as compared to the JK-1 as a result of extended π-conjugation, which is consistent with the absorption spectra of the JK-2 sensitizer. Under standard global AM 1.5 solar condition, the JK-2 sensitized cell gave a short circuit photocurrent density (i_{sc}) of 14.0 ± 0.20 mA/cm^2, an open circuit voltage of 753 ± 10 mV, and a fill factor of 0.77 ± 0.02, corresponding to an overall conversion efficiency η, derived from the equation $\eta = i_{sc} \cdot V_{oc} \cdot$ff/light intensity, of 8.01% (see Figure 7). By contrast, the JK-1 sensitized cell gave a short circuit photocurrent density (i_{sc}) of 12.20 ± 0.20 mA/cm^2, an open circuit voltage of 764 ± 10 mV, and a fill factor of 0.77 ± 0.02, corresponding to an overall conversion efficiency, η, of 7.20%. The lower efficiency of the JK-1 (∼11%) as compared to the JK-2 sensitizer demonstrates the beneficial influence of thiophene units on the photocurrent, due to the enhanced red response.

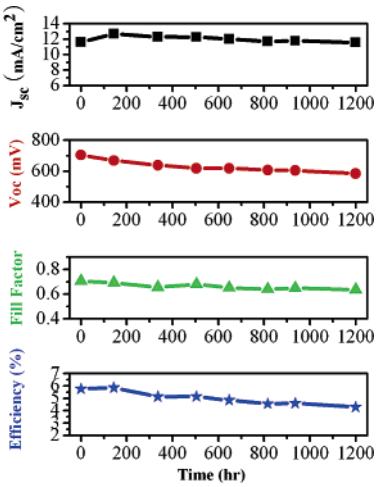

Figure 8. Photovoltaic parameter (J_{sc}, V_{oc}, ff, and η) variations with aging time for the device based on (6 + 4) μm film sensitized with JK-2 and ionic liquid electrolyte during successive 1 sun visible-light soaking at 60 °C.

Figure 8 shows the photovoltaic performance during a long-term accelerated aging of a JK-2 sensitized solar cell using an ionic liquid electrolyte in a solar simulator at full intensity (100 mW cm^{-2}) and 60 °C.[31] Values for the short-circuit current (J_{sc}), open-circuit potential (V_{oc}), fill factor (ff), and overall efficiency (η) were recorded over a period of 1200 h. During the aging process J_{sc} remained practically constant at 11.6 mA/cm^2, while V_{oc} decreased by 120 mV. The overall efficiency remained at 80% of the initial value after 1200 h of light soaking at 60 °C. This 20% decrease reflects mainly the drop in V_{oc} as the change in ff is small. The decrease in V_{oc} is due to an enhancement of the dark current and is presently further investigated. The stability of the photocurrent is remarkable. Using an average for J_{sc} of 11.5 mA/cm^2, the total charge passed through 1 cm^2 surface area during 1200 h of light soaking is 49 680 Coulomb. Using a surface concentration of 10^{-7} mol/cm^2 for the sensitizer, one derives a turnover number of 4.97 million, which the JK-2 dye sustains without any noticeable decline in performance. This demonstrates that the amount of dye on the TiO_2 surface remained intact after light soaking at 60 °C. To the best of our knowledge, this is the first time that organic dyes-based solar cells have been subjected to stability testing under light soaking and thermal stress at 60 °C over such a long period.

Conclusion

In summary, we have molecularly engineered a highly efficient novel type of organic sensitizers, yielding 91% IPCE and 8.01% power conversion efficiency under standard AM 1.5 solar condition. Our finding demonstrates that incorporating thiophene units, bridging the donor and acceptor groups, can systematically control the spectral response and the molar extinction coefficient of the dyes. Further, we have used ionic liquid-based electrolytes giving over 5.8% conversion efficiency to test the stability of the sensitizer under light soaking at 60 °C for 1200 h. The dyes sustained ca. 5 million turnovers without noticeable decline in performance. Work to extend the spectral response of these sensitizers further into the red and near IR spectral region is in progress.

(31) Kuang, D.; Ito, S.; Wenger, B.; Klein, C.; Moser, J.-E.; Humphry-Baker, R.; Zakeeruddin, S. M.; Grätzel, M. *J. Am. Chem. Soc.* **2006**, *128*, 4146−4154.

Experimental Section

Materials and Measurements. UV−vis spectra were recorded in a 1 cm path length quartz cell on a Cary 5 spectrophotometer. Emission spectra were recorded on a Spex Fluorolog 112 using a 90° optical geometry. The emitted light was detected with a Hamamatsu R2658 photomultiplier operated in single photon counting mode. The emission spectra were photometrically corrected using a NBS calibrated 200 W tungsten lamp as reference source.

Electrochemical data were obtained by cyclic voltammetry using a three-electrode cell and an Auto lab System (PGSTAT 30, GPES 4.8 software). The working electrode was a 0.03 cm^2 glassy carbon disk, the auxiliary electrode was a glassy carbon rod, and a silver disk of 0.03 cm^2 was used as quasi-reference electrode. The sensitizers were dissolved in dimethylformamide (DMF) containing 0.1 M tetrabutylammonium hexafluorophosphate as the supporting electrolyte. After the measurement, ferrocene was added as the internal reference for calibration.

Dye-Sensitized Solar Cells. FTO glass plates (Nippon Sheet Glass, Solar 4 mm thickness) were cleaned in a detergent solution using an ultrasonic bath for 15 min, rinsed with water and ethanol, and then treated in a UV-O_3 system for 20 min. The FTO glass plates were immersed in 40 mM $TiCl_4$ (aqueous) at 70 °C for 30 min and washed with water and ethanol. A paste[24] composed of 20 nm anatase TiO_2 particles for the transparent nanocrystalline layer was coated on the FTO glass plates by screen printing, and then dried for 6 min at 125 °C. This coating−drying procedure was repeated to increase the thickness to that required. After the nanocrystalline TiO_2 layer was dried at 125 °C and the thickness of the transparent layer was measured by using an Alpha-step 200 surface profilometer (Tencor Instruments, San Jose, CA), a paste for the scattering layer containing 400 nm sized anatase particles (CCIC, HPW-400) was deposited by twice screen printing.[24] The resulting layer was composed of 10 μm thickness of transparent layer and 4 μm thickness of scattering layer. The TiO_2 electrodes were gradually heated under an air flow at 325 °C for 5 min, at 375 °C for 5 min, at 450 °C for 15 min, and at 500 °C for 15 min. The TiO_2 electrodes were treated again by $TiCl_4$ and sintered at 500 °C for 30 min. The TiO_2 electrodes were immersed into the JK-1 and JK-2 solutions (0.5 mM in a mixture of acetonitrile and *tert*-butyl alcohol (volume ratio: 1:1) containing 1 mM 3a,7a-dihydroxy-5b-cholic acid (Cheno)) and kept at room temperature for 4 h. Counter electrodes were prepared by coating with a drop of H_2PtCl_6 solution (2 mg of Pt in 1 mL of ethanol) on a FTO plate (TEC 15/2.2 mm thickness, Libbey-Owens-Ford Industries) and heating at 400 °C for 15 min. The dye-adsorbed TiO_2 electrode and Pt-counter electrode were assembled into a sealed sandwich-type cell by heating with a hot-melt ionomer film (Surlyn 1702, 25 μm thickness, Du-Pont) as a spacer between the electrodes. A drop of electrolyte solution (electrolyte of 0.6 M *M*-methyl-*N*-butyl imidiazolium iodide, 0.04 M iodine, 0.025 M LiI, 0.05 M guanidinium thiocyanate, and 0.28 M *tert*-butylpyridine in a 15/85 (v/v) mixture of valeronitrile and acetonitrile) was placed on the drilled hole in the counter electrode of the assembled cell and was driven into the cell via vacuum backfilling. Finally, the hole was sealed using additional Bynel and a cover glass (0.1 mm thickness). An antireflection and UV-cut off film (λ < 380 nm, ARKTOP, ASAHI GLASS) was attached to the DSC surface. To reduce scattered light from the edge of the glass electrodes of the dyed TiO_2 layer, light shading masks were used onto the DSSCs, so the active area of DSSCs was fixed to 0.158 cm^2. For the stability test, 6 + 4 μm TiO_2 layers were used, and the ionic liquid composed of 0.2 M iodine, 0.5 M NMBI, and 0.1 M GuNCS in a mixture of PMII/EMINCS (13:7 vol. ratio) was incorporated.[30]

For photovoltaic measurements of the DSSCs, the irradiation source was a 450 W xenon light source (Osram XBO 450, USA), whose power of an AM 1.5 solar simulator was calibrated by using a reference Si photodiode equipped with an IR-cutoff filter (KG-3, Schott) to reduce the mismatch in the region of 350−750 nm between the simulated light

and AM 1.5 to less than 2%.[23] The measurement delay time of photo $I-V$ characteristics of DSSCs was fixed to 40 ms. The measurement of incident photon-to-current conversion efficiency (IPCE) was plotted as a function of excitation wavelength by using the incident light 300 W xenon lamp (ILC Technology, USA), which was focused through a Gemini-180 double monochromator (Jobin Yvon Ltd., UK).

Synthesis of Sensitizers. All experiments were performed under a nitrogen atmosphere in a vacuum atmospheres drybox or by standard Schlenk techniques. THF and toluene were distilled from sodium benzophenone. *N*,*N*-Dimethylformamide (DMF) and acetonitrile were dried and distilled from CaH_2. The ^1H and ^{13}C NMR spectra were recorded on a Varian Gemini 300 spectrometer operating at 300.00 and 75.44 MHz, respectively. Chemical shifts were referenced relative to TMS and H_3PO_4. The IR spectra were recorded on a Biorad FTS-165 spectrometer. Mass spectra were recorded on a JEOL JMS-SX102A instrument. Elemental analyses were performed with a Carlo Erba Instruments CHNS-O EA 1108 analyzer. 2-[*N*,*N*-Bis(9,9-dimethylfluorene-2-yl)phenyl]thiophene[32] and 5-[*N*,*N*-bis(9,9-dimethylfluorene-2-yl)phenyl]-2,2′-bisthiophene[32] were synthesized according to procedures reported in the literature.

5-[*N*,*N*-Bis(9,9-dimethylfluorene-2-yl)phenyl]-thiophene-2-carbaldehyde. To 2-[*N*,*N*-bis(9,9-dimethylfluorene-2-yl)phenyl]thiophene (0.85 g, 1.52 mmol) in *N*,*N*-dimethylformamide (DMF) was added phosphorus oxychloride (0.17 mL, 1.82 mmol) at 0 °C. The solution was warmed to room temperature and stirred for an additional 2 h. After removal of DMF in vacuo, the reaction mixture was neutralized with sodium acetate and extracted with methylene chloride. The crude product was purified by column chromatography using a mixture of ethyl acetate and *n*-hexane (1:10) as an eluent (yield 81%). ^1H NMR ($CDCl_3$, 300 MHz): δ 9.87 (s, 1H), 7.72 (d, 1H), 7.67 (d, 2H), 7.64 (d, 2H), 7.57 (d, 2H), 7.41 (d, 2H), 7.36−7.33 (m, 2H), 7.31 (m, 2H), 7.28 (d, 1H), 7.25 (s, 1H), 7.20 (d, 2H), 7.15 (d, 2H), 1.43 (s, 12H). ^{13}C NMR ($CDCl_3$, 75.44 MHz): δ 182.5, 155.4, 153.7, 149.4, 146.6, 141.3, 138.9, 137.9, 135.2, 134.7, 127.4, 127.2, 126.9, 123.9, 123.0, 122.9, 122.7, 120.9, 120.8, 119.7, 119.4, 47.0, 27.2. FAB MS(*m*/*z*): 587.16 (M^+). Anal. Calcd for $C_{41}H_{33}NOS$: C, 83.78; H, 5.66. Found: C, 83.65; H, 5.52.

3-{5-[*N*,*N*-Bis(9,9-dimethylfluorene-2-yl)phenyl]-thiophene-2-yl}-2-cyano-acrylic Acid. The resulting carbaldehyde thiophene (0.50 g, 0.85 mmol) and cyanoacetic acid (0.09 g, 1.02 mmol) were allowed to react in acetonitrile in the presence of piperidine (0.04 mL, 0.43 mmol). The solution was refluxed for 6 h. After removal of acetonitrile in vacuo, the crude product was extracted with methylene chloride and water. The crude product was purified by column chromatography using methanol as an eluent to give yellow solid product 3-{5-[*N*,*N*-bis(9,9-dimethylfluorene-2-yl)phenyl]-thiophene-2-yl}-2-cyano-acrylic acid (0.41 g, 0.63 mmol, yield 74%). Mp: 242 °C. ^1H NMR (CD_3OD-d_4, 300 MHz): δ 8.16 (s, 1H), 7.70 (d, 2H), 7.68 (d, 2H), 7.64 (d, 2H), 7.44 (d, 2H), 7.43 (d, 2H), 7.30 (d, 2H), 7.27 (s, 2H), 7.24 (d, 2H), 7.16 (d, 2H), 7.12 (d, 2H), 1.41 (s, 12H). ^{13}C NMR (CD_3OD-d_4, 75.44 MHz): δ 171.1, 156.6, 154.9, 152.3, 149.5, 148.2, 140.0, 138.3, 136.4, 131.1, 130.0, 128.2, 127.9, 125.1, 124.1, 123.6, 122.5, 121.9, 121.4, 120.6, 120.4, 119.6, 107.5, 106.6, 30.1, 27.4. FAB MS(*m*/*z*): 654.14 (M^+). Anal. Calcd for $C_{44}H_{34}N_2O_2S$: C, 80.70; H, 5.23. Found: C, 80.57; H, 5.17.

5′-[*N*,*N*-Bis(9,9-dimethylfluorene-2-yl)phenyl]-2,2′-bisthiophene-5-carbaldehyde. To a stirred solution of 5-[*N*,*N*-bis(9,9-dimethylfluorene-2-yl)phenyl]-2,2′-bisthiophene (0.70 g, 1.09 mmol) in *N*,*N*-dimethylformamide (DMF) was added phosphorus oxychloride (0.12 mL, 1.31 mmol) at 0 °C. The solution was warmed to room temperature and stirred for an additional 2 h. After removal of DMF in vacuo, the reaction mixture was neutralized with sodium acetate and extracted with methylene chloride. The crude product was purified by column chromatography using a mixture of ethyl acetate and *n*-hexane (1:5) as an eluent (yield 82%). ^1H NMR ($CDCl_3$, 300 MHz): δ 9.86 (s, 1H), 7.67 (d, 1H), 7.66 (d, 1H), 7.62 (d, 2H), 7.50 (d, 2H), 7.40 (d, 2H), 7.34−7.33 (m, 3H), 7.30 (t, 2H), 7.29 (d, 1H), 7.25 (d, 2H), 7.22−7.18 (m, 4H), 7.13 (d, 2H), 1.36 (s, 12H). ^{13}C NMR ($CDCl_3$, 75.44 MHz): δ 182.6, 155.3, 153.7, 148.3, 147.6, 146.9, 146.4, 141.3, 138.9, 137.7, 134.8, 134.2, 127.4, 127.3, 127.2, 126.8, 126.7, 123.9, 123.6, 123.5, 123.3, 122.7, 120.8, 119.6, 119.1, 46.9, 27.1. FAB MS(*m*/*z*): 669.13 (M^+). Anal. Calcd for $C_{45}H_{35}NOS_2$: C, 80.68; H, 5.27. Found: C, 80.59; H, 5.15.

3-{5′-[*N*,*N*-Bis(9,9-dimethylfluorene-2-yl)phenyl]-2,2′-bisthiophene-5-yl}-2-cyano-acrylic Acid. The resulting carbaldehyde bithophene (0.40 g, 0.60 mmol) and cyanoacetic acid (0.06 g, 0.72 mmol) were allowed to react in acetonitrile in the presence of piperidine (0.03 mL, 0.30 mmol). The solution was refluxed for 6 h. After removal of acetonitrile in vacuo, the crude product was extracted with methylene chloride and water. The crude product was purified by column chromatography using methanol as an eluent to give red solid product 3-{5′-[*N*,*N*-bis(9,9-dimethylfluorene-2-yl)phenyl]-2,2′-bisthiophene-5-yl}-2-cyano-acrylic acid (0.31 g, 0.42 mmol, yield 70%). Mp: 249 °C. ^1H NMR (CD_3OD-d_4, 300 MHz): δ 8.14 (s, 1H), 7.68 (d, 4H), 7.62 (d, 1H), 7.59 (d, 2H), 7.43 (d, 2H), 7.38 (d, 1H), 7.34−7.31 (m, 4H), 7.29−7.26 (m, 4H), 7.15 (d, 2H), 7.11 (d, 2H), 1.41 (s, 12H). ^{13}C NMR (CD_3OD-d_4, 75.44 MHz): δ 169.4, 156.5, 154.8, 150.8, 149.6, 148.4, 140.1, 137.1, 136.1, 135.7, 135.1, 131.9, 129.5, 129.3, 128.9, 128.2, 127.8, 127.6, 126.1, 125.1, 124.6, 123.6, 121.7, 120.5, 120.2, 119.3, 107.8, 106.9, 30.7, 27.4. FAB MS(*m*/*z*): 736.12 (M^+). Anal. Calcd for $C_{48}H_{36}N_2O_2S_2$: C, 78.23; H, 4.92. Found: C, 78.11; H, 4.81.

Acknowledgment. We acknowledge financial support of this work by the KOSEF via the National Research Laboratory (NRL) program (Korea), the Swiss Federal Office for Energy (OFEN), and Institute for Information Technology Advancement (Korea). We thank Dr. Shaik M. Zakeeruddin and Dr. Peter Péchy for providing electrolyte solutions, and Dr. Robin Humphry-Baker, Dr. S. Seigo Ito, Dr. Paul Liska, and Pascal Comte for their kind assistance.

Supporting Information Available: Complete ref 25. This material is available free of charge via the Internet at http://pubs.acs.org.

JA066376F

(32) Kim, S.; Song, K.-H.; Kang, S. O.; Ko, J. *Chem. Commun.* **2004**, 68−69.